Journal of Inorganic Biochemistry 104 (2010) 523–532

Contents lists available at ScienceDirect

Journal of Inorganic Biochemistry

journal homepage: www.elsevier.com/locate/jinorgbio

Synthesis, characterization and cytotoxic activity of gallium(III) complexes anchored by tridentate pyrazole-based ligands

Francisco Silva [a], Fernanda Marques [a], I.C. Santos [a], António Paulo [a], António Sebastião Rodrigues [b], José Rueff [b], Isabel Santos [a,*]

[a] Unidade de Ciências Químicas e Radiofarmacêuticas, Instituto Tecnológico e Nuclear, Estrada Nacional 10, 2686-953 Sacavém, Portugal
[b] CIGMH, Department of Genetics, Faculty of Medical Sciences, New University of Lisbon, Rua da Junqueira 96, 1349-008 Lisboa, Portugal

ARTICLE INFO

Article history:
Received 5 July 2009
Received in revised form 5 January 2010
Accepted 11 January 2010
Available online 20 January 2010

Keywords:
Gallium(III) complexes
Pyrazole-based ligands
X-ray structures
Cytotoxicity
Apoptosis

ABSTRACT

Reactions of $GaCl_3$ with pyrazole-containing ligands of the pyrazole-imine-phenol (**HL^1**–**HL^3**) or pyrazole-amine-phenol (**HL^4**–**HL^6**) types led to the synthesis of well-defined $[GaL_2]^+$ homoleptic complexes (**1**–**6**). Complexes **1**–**6** were characterized by elemental analysis, ESI-MS (electrospray ionization-mass spectrometry), IR and NMR spectroscopies, and in the case of Complex **1** also by X-ray diffraction analysis. In complexes **1**–**3**, the pyrazole-imine-phenolate ligands act as monoanionic chelators that coordinate to the metal in a meridional fashion, while **4**–**6** contain monoanionic and facially coordinated pyrazole-amine-phenolate ligands. Complexes **1**–**3** have a greater stability in solution compared to **4**–**6**, which have shown a more pronounced tendency to release the respective ancillary ligands. The cytotoxicity of **1**–**6** and of the respective ligands (**HL^1**–**HL^6**) was evaluated against human prostate cancer cells PC-3 and human breast cancer cells MCF-7. The substituents of the phenolate rings strongly influenced the cytotoxicity of the compounds. Complexes **3** and **6** that contain chloride substituents at the phenolate rings have shown the highest cytotoxicity, including in the cisplatin-resistant PC-3 cell line. The cytotoxic profile of **3** and **6** is very similar to the one displayed by the respective anchor ligands, respectively **HL^1** and **HL^6**. The cytotoxic activity of **3** and **6** is slightly increased by the presence of transferrin, and both complexes provoke cell death mainly by induction of apoptotic pathways.

1. Introduction

The clinical success of cisplatin in the treatment of several human malignant tumors motivated in recent years strong research efforts on the finding of alternative metal complexes with potential usefulness as anticancer drugs [1]. So far, some of the most promising results have been reported for gallium, which exhibits antineoplastic activity even in the form of simple Ga(III) salts, such as the nitrate or chloride. However, the use of Ga(III) salts as anticancer drugs presents some drawbacks, which are mainly related with their toxicity and relatively poor bioavailability. To overcome these limitations and seeking for compounds with more favorable pharmacokinetics, Ga(III) complexes anchored by multidentate chelators started to be evaluated in recent years as alternatives to gallium salts. In particular, the complexation of Ga(III) by multidentate chelators is expected to prevent hydrolysis processes, while improving bioavailability and cell membrane permeation of the compounds [1,2].

In recent years, the search for Ga(III) complexes potentially useful as anticancer drugs has been based on bidentate and tridentate chelators, containing aromatic or N-heterocyclic rings and combining different donor atoms such as nitrogen, sulfur and oxygen. So far, the more promising results were reported for tris(-8-quinolinolato)gallium(III) (KP46) and tris(3-hydroxy-2-methyl-4H-pyran-4-onato)gallium(III), two neutral complexes anchored by bidentate donors that are currently undergoing clinical evaluation [1,2]. Compared to gallium salts, several monocationic and homoleptic Ga(III) complexes anchored by tridentate chelators have also presented an enhanced cytotoxic activity against human tumor cells, namely cisplatin-resistant cell lines [3–8]. Although the mechanisms involved in the anticancer activity of Ga(III) complexes are not fully understood, it is generally considered that the critical cellular target of gallium is the enzyme ribonucleotide reductase [1]. More recently, it has been shown that cationic Ga(III) complexes with N,N′O-donors, containing pyridine, amine and phenolate coordinating groups, can act as potent inhibitors of the proteasome activity, which emerged therefore as a novel therapeutic target of gallium-based anticancer agents [9]. All together, these results point out that Ga(III) complexes with tridentate chelators deserve to be further investigated as cytotoxic agents. In this context, the

* Corresponding author.
E-mail address: isantos@itn.pt (I. Santos).

0162-0134/$ - see front matter © 2010 Elsevier Inc. All rights reserved.
doi:10.1016/j.jinorgbio.2010.01.003

finding of compounds with improved pharmacological and pharmacokinetics properties and the understanding of the mechanisms that are involved on their antiproliferative action are still very important issues in contemporary inorganic medicinal chemistry.

In this contribution, we report on the synthesis and characterization of cationic and homoleptic Ga(III) complexes (**1**–**6**) anchored by (N, N′, O) pyrazolyl-containing chelators, as well as on the evaluation of their interest as cytotoxic metallopharmaceuticals. As shown in Fig. 1, we have explored pyrazolyl-imine-phenolate ligands (**HL^1**–**HL^3**) and the respective pyrazolyl-amine-phenolate congeners (**HL^4**–**HL^6**). By choosing these ligands, we expected to clarify how the rigidity and ring substituents would influence the structure, stability and cytotoxic activity of the corresponding Ga(III) complexes (**1**–**6**) of the $[GaL_2]^+$ type.

Complexes **1**–**6** were characterized by the common analytical techniques, including multinuclear (^{1}H, ^{13}C and ^{71}Ga) NMR in the case of **1**–**3** and X-ray diffraction analysis for **1**. The biological evaluation of the ligands **HL^1**–**HL^6** and complexes **1**–**6** comprised the screening of their *in vitro* cytotoxic activity in the human cancer cell lines MCF-7 and PC-3. For the more cytotoxic complexes, their ability to induce apoptosis and the influence of transferrin on their cytotoxic activity were also studied and will be reported herein.

2. Experimental section

2.1. General procedures

The syntheses were carried under a nitrogen atmosphere, using standard Schlenk techniques and dry solvents, while the work-up procedures were performed under air. The compounds N-(2-aminoethyl)pyrazole, N-(2-hydroxybenzyl-2-pyrazolethyl)imine (**HL^1**) and N-(2-hydroxybenzyl-2-pyrazolethyl)amine (**HL^4**) were prepared according to the procedures described in the literature [10,11]. ^{1}H and ^{13}C NMR spectra were recorded in a Varian Unity 300 MHz spectrometer and ^{71}Ga NMR spectra in a Bruker Avance-500 MHz NMR spectrometer. ^{1}H and ^{13}C chemical shifts (ppm) were referenced with the residual solvent resonances relative to tetramethylsilane. The ^{71}Ga NMR spectra were recorded in ppm relative to a $Ga(NO_3)_3$ external reference in D_2O. IR spectra were recorded as KBr pellets on a Bruker Tensor 27 spectrometer. C, H and N analyzes were performed on an EA 110 CE instruments automatic analyzer. Electrospray ionization-mass spectrometry (ESI-MS) of complexes **1**–**6** was carried out with a QITMS instrument, using acetonitrile solutions of the compounds.

2.2. Synthesis of the ligands

The new pyrazole-imine-phenolate ligands **HL^2 and HL^3** were synthesized and purified as previously described for the congener **HL^1** by reacting N-2-(aminoethyl)pyrazole with an equivalent amount of the respective salicilaldeyde, in dry EtOH under reflux for 2 h [11]. **HL^2** and **HL^3** were isolated as yellow microcrystalline solids, after removing the solvent under vacuum and washing the residue with *n*-hexane and diethyl ether. The corresponding amines, **HL^5** and **HL^6**, were obtained by reduction of **HL^2** and **HL^3** with a twofold excess of $NaBH_4$ in dry methanol, as we have previously reported for **HL^4**. The purification of **HL^5** and **HL^6** was done by evaporation of methanol, redissolution of the residue in CH_2Cl_2 and washing of the organic solution with aqueous K_2CO_3. **HL^5** and **HL^6** were isolated as yellow microcrystalline solids after removal of dichoromethane and washing of the obtained residue with *n*-hexane.

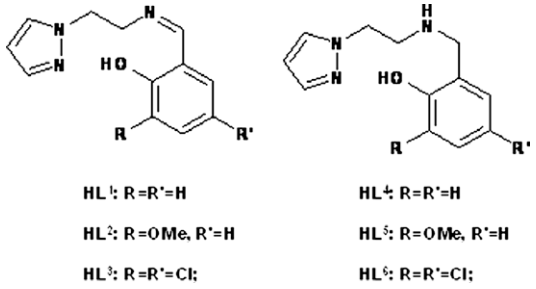

Fig. 1. Ligands of the pyrazole-imine-phenol (**HL^1**–**HL^3**) and pyrazole-amine-phenol (**HL^4**–**HL^6**) type used in this work to prepare homoleptic Ga(III) complexes.

2.2.1. N-(2-hydroxy-3-methoxy-benzyl-2-pyrazolethyl)imine (*HL^2*)

Starting from 0.1 g (0.9 mmol) of N-2-(aminoethyl)pyrazole were obtained 0.163 g (0.66 mmol) of **HL^2**. Yield: 74%. Element. Anal. (%). Found: C, 62.85; N, 17.09; H, 7.17; Calc. for $C_{13}H_{15}N_3O_2$?0.1 H_2O: C, 63.19; N, 17.01 H, 6.20. IR (KBr, cm^{-1}): 1630 ($\upsilon_{C=N}$), 3125 (υ_{O-H}). ^{1}H NMR δ_H (300 MHz, $CDCl_3$, s = singlet, d = doublet, m = multiplet, tr = triplet): 13.36 (1H, s, OH), 8.04 (1H, s, N═CH), 7.51 (1H, d, H(3/5)-pz), 7.33 (1H, d, H(3/5)-pz), 6.89 (1H, m, Ph), 6.83 (1H, m, Ph), 6.75 (1H, m, Ph), 6.13 (1H, tr, H(4)-pz), 4.34 (2H, tr, N—CH_2), 4.04 (2H, pz-CH_2), 3.89 (3H, s, O–CH_3). ^{13}C NMR δ_C (75.4 MHz, $CDCl_3$): 167.81 (N═CH), 150.93 (Ph), 148.04 (Ph), 140.86 (C(3/5)-pz), 130.56 (Ph + C(3/5)-pz), 118.32 (Ph), 113.98 (Ph), 105.02 (C(4)-pz), 58.74 (CH_2), 56.05 (CH_3–O), 52.18 (CH_2).

2.2.2. N-(2-hydroxy-3,5-dichloride-benzyl-2-pyrazolethyl)imine (*HL^3*)

Starting from 0.2 g (1.8 mmol) of N-2-(aminoethyl)pyrazole were obtained 0.45 g (1.58 mmol) of **HL^3**. Yield: 88%. Element. Anal. (%). Found: C, 48.07; N, 13.46; H, 3.78. Calc. for $C_{12}H_{11}N_3OCl_2$?H_2O: C, 47.70; N, 13.91; H, 4.34. IR (KBr, cm^{-1}): 1620 ($\upsilon_{C=N}$), 3100 (υ_{O-H}). ^{1}H NMR δ_H (300 MHz, $CDCl_3$): 13.87 (1H, s, OH), 7.85 (1H, s, N═CH), 7.48 (1H, d, H(3/5)-pz), 7.26 (1H, d, H(3/5), pz), 7.25 (1H, m, Ph), 6.96 (1H, m, Ph), 6.12 (1H, tr, H(4)-pz), 4.39 (2H, tr, N—CH_2), 4.03 (2H, pz-CH_2). ^{13}C NMR δ_C (75.4 MHz, $CDCl_3$): 166.45 (N═CH), 155.98 (Ph), 140.93 (C(3/5)-pz), 131.04 (Ph + C(3/5)-pz), 133.36 (Ph), 124.67 (Ph), 119.14 (Ph), 105.41 (C(4)-pz), 58.24 (CH_2), 51.77 (CH_2).

2.2.3. N-(2-hydroxybenzyl-3-methoxy-2-pyrazolethyl)amine (*HL^5*)

Starting from 0.1 g (0.41 mmol) of **HL^2** were obtained 0.081 g (0.33 mmol) of **HL^5**. Yield: 80%. Element. Anal. (%). Found: C, 61.38; N, 15.84; H, 6.24. Calc. for $C_{13}H_{17}N_3O_2$?0.5 H_2O: C, 60.92; N, 16.39; H, 7.08. IR (KBr, cm^{-1}): 3300 (υ_{N-H}), 3090 (υ_{O-H}). ^{1}H NMR δ_H (300 MHz, $CDCl_3$): 7.52 (1H, d, H(3/5)-pz), 7.39 (1H, d, H(3/5)-pz), 6.81 (1H, m, Ph), 6.74 (1H, m, Ph), 6.58 (1H, m, Ph), 6.24 (1H, tr, H(4)-pz), 4.26 (2H, tr, pz-CH_2), 3.98 (2H, s, N—CH_2), 3.86 (3H, s, O–CH_3), 3.09 (2H, tr, N—CH_2). ^{13}C NMR δ_C (75.4 MHz, $CDCl_3$): 147.96 (Ph), 146.98 (Ph), 140.07 (C(3/5)-pz), 129.99 (Ph + C(3/5)-pz), 115.42 (Ph), 110.52 (Ph), 105.53 (C(4)-pz), 55.97 (CH_3–O), 51.56 (CH_2), 51.07 (CH_2), 47.78 (CH_2).

2.2.4. N-(2-hydroxybenzyl-3,5-dichloride-2-pyrazolethyl)amine (*HL^6*)

Starting from 0.227 g (0.8 mmol) of **HL^3** were obtained 0.192 g (0.67 mmol) of **HL^6**. Yield: 84%. Element. Anal. (%). Found: C, 48.07; N, 13.46; H, 3.78. Calc. for $C_{12}H_{13}N_3OCl_2$?0.9 H_2O: C, 47.67; N, 13.90; H, 4.93. IR (KBr, cm^{-1}): 3200 (υ_{N-H}), 3125 (υ_{O-H}). ^{1}H NMR δ_H (300 MHz, $CDCl_3$): 7.52 (1H, d, H(3/5)-pz), 7.39 (1H, d, H(3/5)-pz), 6.87 (1H, m, Ph), 6.85 (1H, Ph), 6.27 (1H, tr, H(4)-pz), 4.26 (2H, d, pz-CH_2), 3.96 (2H, s, N—CH_2), 3.08 (2H, N—CH_2). ^{13}C NMR δ_C (75.4 MHz, $CDCl_3$): 152.70 (Ph), 139.96 (C(3/5)-pz), 130.75 (Ph + C(3/5)-pz), 126.87 (Ph), 124.64 (Ph), 121.60 (Ph), 105.79 (C(4)-pz), 52.09 (CH_2), 50.52 (CH_2), 47.77 (CH_2).

2.3. Synthesis of the gallium complexes

2.3.1. General procedure for the synthesis of Complexes **1**–**3** and **5**

Inside a nitrogen-filled glove-box, a solution of the desired ligand (L) and NEt_3 in dry methanol was stirred at room temperature for 30 min. Then, solid $GaCl_3$ was added and the resulting solution was stirred for 1 h at room temperature. NH_4PF_6 was added and the mixture was stirred for another hour. The Ga complexes precipitated as microcrystalline solids, which were recovered by centrifugation, washed with cold methanol and dried under vacuum. The syntheses were performed using a 2:2:1:1 (L:NEt_3:-$GaCl_3$:NH_4PF_6) molar ratio of the reagents.

2.3.2. General procedure for the synthesis of Complexes **4** and **6**

Inside a nitrogen-filled glove-box, a solution of the desired ligand (L) and an equimolar amount of NEt_3 in dry methanol was stirred at room temperature for 30 min. Then, one-half equivalent of solid $GaCl_3$ was added and the resulting solution was stirred for 1 h at room temperature. After this time, the complexes precipitated as microcrystalline solids that were recovered by centrifugation, washed with cold methanol and dried under vacuum.

2.3.3. Gallium(III) bis[N-(2-hydroxybenzyl-2-pyrazolethyl)imine] hexafluorophosphate (**1**)

Starting from 0.041 g (0.23 mmol) of $GaCl_3$ were obtained 0.096 g (0.15 mmol) of complex $[Ga(L^1)_2]PF_6$ (**1**) in the form of a white microcrystalline solid. Yield: 65%. Element. Anal (%). Found: C, 44.86; N, 13.47; H, 3.10. Calc. for $C_{24}H_{24}GaN_6O_2PF_6$: C, 44.82; N, 13.07; H, 3.76. ESI-MS: (*m/z*): Found: 497.0 $[M]^+$. Calc: 497.1 $[M]^+$. IR (KBr, cm^{-1}): 1625 ($\upsilon_{C=N}$). ^1H NMR δ_H (300 MHz, CD_3CN): 8.48 (2H, s, N═CH), 7.66 (2H, d, H(3/5),pz), 7.26 (6H, m, Ph + H(3/5)-pz), 6.27 (4H, m, Ph), 6.22 (2H, tr, H(4)-pz), 5.01 (2H, br, N—CH_2), 4.61 (2H, N—CH_2), 4.33 (4H, pz-CH_2). ^{13}C NMR δ_C (75.4 MHz, CD3CN): 174.79 (N═CH), 167.36 (Ph), 140.21 (C(3/5)-pz), 137.32 (Ph + C(3/5)-pz), 134.45 (Ph), 123.18 (Ph) 117.33 (Ph) 106.73 (C(4)-pz), 59.99 (CH_2), 50.44 (N—CH_2). ^{71}Ga NMR δ_{Ga} (152.5 MHz, CD_3CN): 24.07.

2.3.4. Gallium(III) bis[N-(2-hydroxy-3-methoxy-benzyl-2-pyrazolethyl)imine] hexafluorophosphate (**2**)

Starting from 0.027 g (0.15 mmol) of $GaCl_3$ were obtained 0.057 g (0.08 mmol) of complex $[Ga(L^2)_2]PF_6$ (**2**) in the form of a greenish microcrystalline solid. Yield: 54%. Element. Anal (%). Found: C, 43.25; N, 11.74; H, 4.93. Calc. for $C_{26}H_{28}GaN_6O_4PF_6?H_2O$: C, 43.30; N, 11.65; H, 4.19. ESI-MS: (*m/z*): Found: 557.0 $[M]^+$. Calc: 557.1 $[M]^+$. IR (KBr, cm^{-1}): 1620 ($\upsilon_{C=N}$). ^1H NMR δ_H (300 MHz, CD_3CN): 8.46 (2H, s, N═CH), 7.65 (2H, d, H(3/5)-pz), 7.24 (2H, d, H(3/5)-pz), 6.92 (2H, m, Ph), 6.64 (2H, m, Ph), 6.57 (2H, m, Ph), 6.20 (2H, tr, H(4)-pz), 5.36 (2H, br, N—CH_2), 4.55 (2H, br, N—CH_2), 4.32 (4H, br, pz-CH_2), 3.73 (4H, O–CH_3). ^{13}C NMR δ_C (75.4 MHz, CD3CN): 178.99 (N═CH), 162.34 (Ph), 156.63 (Ph), 144.47 (C(3/5)-pz), 139.03 (Ph + C(3/5)-pz), 125.56 (Ph), 120.81 (Ph), 110.93 (C(4)-pz), 64.21 (pz-CH_2), 60.58 (OCH_2), 54.33 (N—CH_2). ^{71}Ga NMR δ_{Ga} (152.5 MHz, CD_3CN): 27.99.

2.3.5. Gallium(III) bis[N-(2-hydroxy-3,5-dichloride-benzyl-2-pyrazolethyl)imine] hexafluorophosphate (**3**)

Starting from 0.019 g (0.11 mmol) of $GaCl_3$ were obtained 0.039 g (0.05 mmol) of complex $[Ga(L^3)_2]PF_6$ (**3**) in the form of a greenish microcrystalline solid. Yield: 45%. Element. Anal (%). Found: C, 36.45; N, 10.95; H, 2.25. Calc. for $C_{24}H_{20}GaN_6O_2Cl_4PF_6{\cdot}0.2H_2O$: C, 36.74; N, 10.71; H, 2.58. ESI-MS: (*m/z*): Found: 634.9 $[M]^+$. Calc: 634.9 $[M]^+$. IR (KBr, cm^{-1}): 1620 ($\upsilon_{C=N}$). ^1H NMR δ_H (300 MHz, CD_3CN): 8.50 (2H, s, N═CH), 7.75 (2H, d, H(3/5)-pz), 7.49 (2H, d, H(3/5)-pz), 7.36 (2H, m, Ph), 7.21 (2H, m, Ph), 6.29 (2H, tr, H(4)-pz), 5.17 (2H, br, N—CH_2), 4.60 (2H, br, N—CH_2), 4.46 (4H, br, pz-CH_2). ^{13}C NMR δ_C (75.4 MHz, CD_3CN): 173.43 (N═CH), 157.52 (Ph), 140.04 (C(3/5)-pz), 132.12 (Ph + C(3/5)-pz), 135.19 (Ph), 123.56 (Ph), 117.78 (Ph), 106.69 (C(4)-pz), 60.09 (pz-CH_2), 49.94 (N—CH_2). ^{71}Ga NMR δ_{Ga} (152.5 MHz, CD_3CN): 25.97.

2.3.6. Gallium(III) bis[N-(2-hydroxybenzyl-2-pyrazolethyl)amine] chloride (**4**)

Starting from 0.032 g (0.18 mmol) of $GaCl_3$ were obtained 0.074 g (0.14 mmol) of complex $[Ga(L^4)_2]Cl$ (**4**) in the form of a white microcrystalline solid. Yield: 76%. Element. Anal (%). Found: C, 50.85; N, 14.57; H, 5.26. Calc. for $C_{24}H_{28}GaN_6O_2Cl?1.7\ H_2O$: C, 50.72; N, 14.79; H, 5.57. ESI-MS (*m/z*): Found: 500.9 $[M]^+$. Calc: 501.1 $[M]^+$. IR (KBr, cm^{-1}): 3125 (υ_{N-H}). ^1H NMR δ_H (300 MHz, DMSO-d_6): 8.35 (2H, br, H(3/5)-pz), 7.86 (2H, br, H(3/5)-pz), 6.95 (2H, m, Ph), 6.86 (2H, m, Ph), 6.56 (2H, d, Ph), 6.42 (2H, br, Ph), 6.15 (2H, H(4)-pz), 5.05 (2H, NH), 4.48 (4H, br, CH_2), 3.75 (4H, br, CH_2).

2.3.7. Gallium(III) bis[N-(2-hydroxy-3-methoxy-benzyl-2-pyrazolethyl)amine] hexafluorophosphate (**5**)

Starting from 0.046 g (0.26 mmol) of $GaCl_3$ were obtained 0.101 g (0.17 mmol) of complex $[Ga(L^5)_2]PF_6$ (**5**) in the form of a white microcrystalline solid. Yield: 65%. Element. Anal (%). Found: C, 42.66; N, 11.40; H, 5.28. Calc. for $C_{26}H_{32}GaN_6O_2PF_6?3.2\ H_2O$: C, 42.61; N, 11.47; H, 5.28. ESI-MS: (*m/z*): Found: 561.0 $[M]^+$. Calc: 561.1 $[M]^+$. IR (KBr, cm^{-1}): 3135 (υ_{N-H}). ^1H NMR δ_H (300 MHz, CD_3CN): 8.01 (2H, br, H(3/5)-pz), 7.55 (2H, br, H(3/5), pz), 6.68 (2H, d, Ph), 6.48–6–43 (4H, m. Ph), 6.18 (2H, br, H(4)-pz), 5.30 (2H, tr, CH_2), 4.83 (2H, br, NH), 4.28 (2H, m, CH_2), 3.89 (2H, m, CH_2), 3.78 (6H, s, O–CH_3), 3.48 (2H, m, CH_2), 3.33 (2H, CH_2), 2.49 (2H, m, CH_2).

2.3.8. Gallium(III) bis[N-(2-hydroxy-3,5-dichloride-benzyl-2-pyrazolethyl)amine] chloride (**6**)

Starting from 0.025 g (0.14 mmol) of $GaCl_3$ were obtained 0.054 g (0.08 mmol) of complex $[Ga(L^6)_2]Cl$ (**6**) in the form of a pale violet microcrystalline solid. Yield: 57%. Element. Anal (%). Found: C, 40.99; N, 11.85; H, 3.00. Calc. for $C_{24}H_{24}GaN_6O_2Cl_5?1.6\ H_2O$: C, 40.93; N, 11.93; H, 3.89. ESI-MS (*m/z*): Found: 638.9 $[M]^+$. Calc: 639.0 $[M]^+$. IR (KBr, cm^{-1}): 3125 (υ_{N-H}). ^1H NMR δ_H (300 MHz, CD_3CN): 8.07 (2H, br, H(3/5)-pz), 7.66 (2H, br, H(3/5)-pz), 7.22 (2H, br, Ph), 6.90 (2H, br, Ph), 6.43 (2H, br, H(4)-pz), 5.24 (2H, tr, CH_2), 4.93 (2H, br, NH), 4.37 (2H, d, CH_2), 3.82 (2H, d, CH_2), 3.63 (2H, m, CH_2), 3.40 (2H, d, CH_2), 2.61 (2H, m, CH_2).

2.3.8.1. X-ray diffraction analysis. The X-ray diffraction analysis of **1** has been performed on a Bruker AXS APEX CCD area detector diffractometer, using graphite monochromated Mo Kα radiation (0.71073 Å). Empirical absorption correction was carried out using SADABS [12]. Data collection and data reduction were done with the SMART and SAINT programs [13]. The structure was solved by direct methods with SIR97 [14] and refined by full-matrix least-squares analysis with SHELXL-97 [15] using the WINGX [16] suite of programmes. All non-hydrogen atoms were refined anisotropically. The remaining hydrogen atoms were placed in calculated positions. Molecular graphics were prepared using ORTEP3 [17]. A summary of the crystal data, structure solution and refinement parameters are given in Table 1.

2.4. Cell viability assays in human tumor cell lines

2.4.1. Experiments with the complexes and respective ligands

The tumor cell lines MCF-7 and PC-3 (ATCC) were cultured in DMEM (Dulbecco's Modified Eagle Medium) containing GlutaMax I (MCF-7) and RPMI 1640 (PC-3) culture medium (Gibco)

Table 1
Crystallographic data for $[Ga(L^1)_2]PF_6$ (**1**).

Chemical formula	$C_{24}H_{24}F_6GaN_6O_2P$
Formula weight	643.18
Crystal system	Monoclinic
Space group	Pn
a/Å	8.3515(5)
b/Å	12.1952(7)
c/Å	12.9603(6)
β/deg	102.345(2)
V(Å^3)	1289.46(12)
Z	2
T/K	150(2)
ρ(calcd.)/gcm^{-3}	1.657
μMoKα mm^{-1}	1.209
θ range for data collection (°)	3.00–25.68
n°of data	3633
n° of params	361
R indices (all data)	R_1 = 0.0295
	wR_2 = 0.0611
R indices [I > 2*σ*(I)]	R_1 = 0.0271
	wR_2 = 0.0600
GOF	0.898

supplemented with 10% FBS and 1% penicillin/streptomycin at 37 °C in a humidified atmosphere of 95% of air and 5% CO_2 (Heraeus, Germany). The cells were adherent in monolayers and, when confluent, were harvested by digestion with 0.05% trypsin–EDTA (Gibco) and seeded farther apart.

Cell viability was evaluated by using a colorimetric method based on the tetrazolium salt MTT ([3-(4,5-dimethylthiazol-2-yl)-2,5-diphenyltetrazolium bromide]), which is reduced by living cells to yield purple formazan crystals. Cells were seeded in 96-well plates at a density of 2×10^4 cells (PC-3) and 5×10^4 cells (MCF-7) per well in 200 μL of culture medium and left to incubate overnight for optimal adherence. After careful removal of the medium, 200 μL of a dilution series of the compounds in fresh medium were added and incubation was performed at 37 °C/5% CO_2 for 24 h or 72 h. **HL^1**–**HL^6** and **1**–**6** were first solubilized in DMSO, diluted in medium and added to the cells in final concentrations between 16 nM and 160 μM. The percentage of DMSO in cell culture medium did not exceed 1%. Cisplatin was first solubilized in saline and then added at the same concentrations used for the other compounds. At the end of the incubation period, the compounds were removed and the cells were incubated with 200 μL of MTT solution (500 μg/ml). After 3–4 h at 37 °C/5% CO_2, the medium was removed and the purple formazan crystals were dissolved in 200 μL of DMSO by shaking. The cell viability was evaluated by measurement of the absorbance at 570 nm by using a plate spectrophotometer (Power Wave Xs, Bio-Tek). The cell viability was calculated dividing the absorbance of each well by that of the control wells (cells treated with medium containing 1% DMSO). Each experiment was repeated at least three times and each point was determined in at least six replicates.

2.4.2. Experiments with the complexes and transferrin

The effect of transferrin on cell viability either as a single agent or in combination with **3** and **6** was evaluated using 100 μg/well of transferrin and increasing concentrations of **3** and **6** (1.6, 16 and 80 μM). MCF-7 or PC-3 cells were plated at a density of 8×10^3 cells (PC-3) and 1.2×10^4 cells (MCF-7) per well in 200 μL of culture medium and were incubated in the presence of the compounds. After 72 h cell viability was evaluated using the MTT assay as described above.

2.5. Apoptosis (annexin assay)

PC-3 cells were seeded in eight well chamber slides (LABTEK, Nalge Nunc Int.) and 24 h later the medium was removed and replaced with fresh one. Compounds **3** and **6**, dissolved in DMSO, were added to the wells and after 24 h the medium was removed, and cells were washed with binding buffer (BB) (HEPES 0,1 M, NaCl 1,4 M, $CaCl_2$ 25 mM, pH = 7,4). The cytotoxic drug taxol (Paclitaxel) was used as a positive control (100 nM). Annexin V (Sigma) (1 μg/ml) and propidium iodide (Chemicon Int) (2 μg/ml) in BB was added to each well for 20 min at 37 °C, in the dark. After this period, cells were washed with BB, and Hoechst 33258 in BB was added (1 μg/ml) for 10 min. Cells were finally washed with BB and mounted with Anti fade Mounting medium (VectaSHIELD® H-1000), and analyzed by fluorescence microscope (LEICA DMLB), equipped with the appropriate filters and attached to a digital camera (applied imaging) and to a personal computer. Images were captured from each slide using Cytovision (v3.0) capture software. Duplicate assays with replicates were performed and at least five different fields were analyzed per dose per experiment.

2.6. Statistical analysis

Statistical analysis was done with GraphPad Prism software to assess if there was a significant difference between the IC_{50} values of complexes **1**–**3** and ligands **HL^1**–**HL^3**. A *p*-value < 0.0001 was considered statistically relevant.

3. Results and discussion

3.1. Synthesis

As depicted in Scheme 1, the novel cationic Ga(III) complexes, **1**–**6**, were obtained by treating gallium(III) chloride with the corresponding ligand in a 1:2 molar ratio, in dry methanol and under basic conditions. Complexes **1**–**3** and **5** were isolated as microcrystalline solids in moderate yield (45–65%) after counter-ion metathesis with sodium hexafluorophosphate. Being less soluble in methanol, **4** and **6** precipitated directly from the respective reaction mixture, and were isolated as chloride salts in moderate to high yield (57–76%). All the isolated compounds (**1**–**6**) are soluble in polar organic solvents like dimethyl sulfoxide, but are only sparingly soluble in water. Their characterization has been done by FT-IR, ^{1}H NMR, ESI-MS and elemental analysis. For some of the compounds, the obtained elemental analysis are somewhat unsatisfactory but the proposed formulations are supported by other analytical data, such as ^{1}H NMR and ESI-MS data. Complexes **1**–**3** were also characterized by ^{13}C and ^{71}Ga NMR, as well as by X-ray diffraction analysis in the case of **1**. The analytical data obtained for **1**–**3**, including good elemental analyzes, were consistent with the presence of pseudo-octahedral $[GaL_2]^+$ complexes. ESI-MS and ^{1}H NMR analysis of **4**–**6** have shown the presence of the same type of homoleptic complexes, but have also indicated the presence of the respective free ligands. As discussed below in more detail, this may reflect the occurrence of dynamic processes in solution, namely of the intermolecular type, and not necessarily the contamination with excess of the ligand.

3.2. Mass spectrometry and spectroscopic characterization

The most significant feature of the IR spectra of complexes **1**–**3** is the presence of ν(C=N) bands in the range 1625–1620 cm^{-1}, undergoing a slightly red shift upon coordination to the metal. The IR spectra of **4**–**6** showed medium intense bands between 3135 and 3125 cm^{-1} that were assigned to ν(N—H) of the coordinated ligands. These frequencies compare well with those that have been reported for other homoleptic Ga(III) complexes anchored by related tridentate ligands containing pyridine and phenoxide coordinating groups [18].

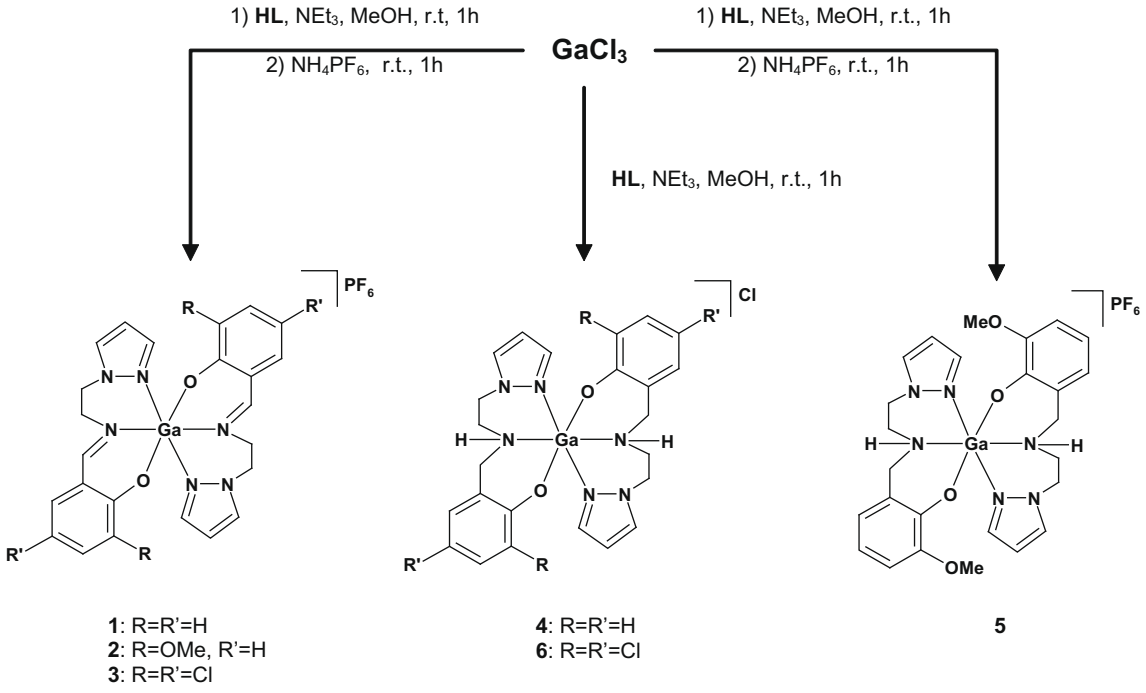

Scheme 1. Synthesis of the Ga(III) complexes.

For **1**–**3** in acetonitrile solution, the ESI mass spectra in the positive mode have shown the presence of prominent peaks corresponding to $m/z = [GaL_2]^+$ with isotopic patterns in agreement with the elemental composition of the complexes. Any other peaks present in the mass spectra of **1**–**3** displayed very low intensity. Under the same conditions, the ESI mass spectrometry analysis of complexes **4**–**6** gave markedly different results, being observed quite intense peaks due the protonated ligands ($m/z = [L + H]^+$). Nevertheless, the molecular-ions corresponding to the homoleptic Ga(III) complexes ($m/z = [GaL_2]^+$) were detected in all the spectra.

Complexes **1**–**3** were studied by multinuclear (^1H, ^{13}C and ^{71}Ga) NMR. In CD_3CN solution, the ^1H NMR and ^{13}C NMR spectra of **1**–**3** are very similar and are consistent with the magnetic equivalence of the two ligands coordinated to the Ga^{3+} ion in a meridional fashion, a coordination mode that was confirmed for **1** in the solid state by X-ray crystallography (see below). As exemplified for Complex **1** in Fig. 2, such magnetic equivalence was easily accounted for by the presence of a unique set of resonances assigned to the aromatic protons, to the imine protons and to the pyrazolyl protons in the ^1H NMR spectra of **1**–**3**. These protons are slightly lowfield shifted ($\Delta\delta$ = 0.1–0.3 ppm) compared to the corresponding protons in the respective free ligands, corroborating the coordination of the phenoxide, imine and pyrazolyl groups to the metal. By contrast, the CH_2 protons from the ethylenic bridge linking the pyrazolyl and imine groups suffer a more pronounced deshielding ($\Delta\delta$ = 0.3–0.6 ppm) upon coordination to the metal. The CH_2 protons adjacent to the imine function originate two broad signals, appearing between 4.55 and 4.61 ppm

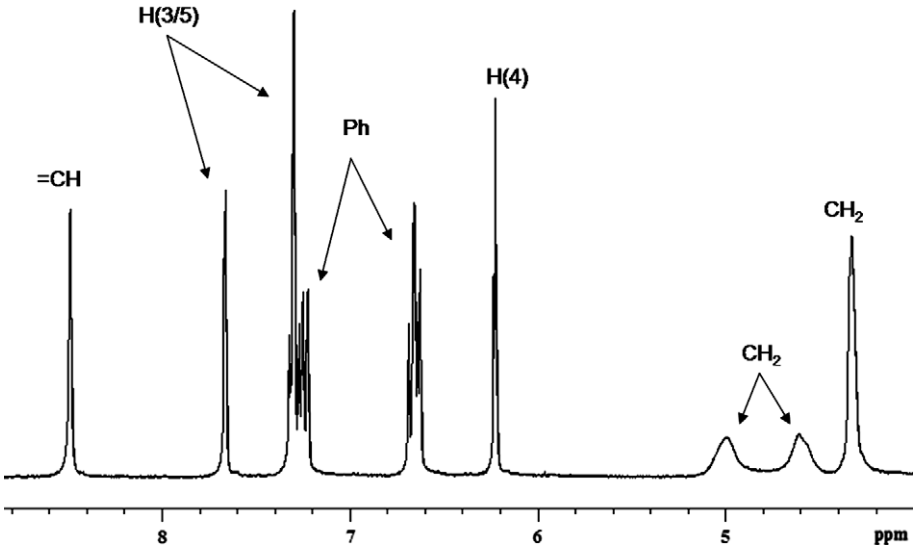

Fig. 2. ^1H NMR spectrum of **1** in CD_3CN.

and integrating each for two protons. The CH_2 protons adjacent to the pyrazolyl ring give rise to a unique broad signal that appears in the range 3.93 and 4.46 ppm and integrates for four protons. The assignment of these CH_2 resonances has been based on the study of **1** by $^1H/^{13}C$ HSQC and on the similarity of the ^1H and ^{13}C NMR spectra of complexes **1**–**3**. These compounds were also studied by ^{71}Ga NMR. The obtained spectra have shown the presence of one relatively broad resonance (see Fig. 3) in the range +22.1/+28.0 ppm. These values are at the low-end of chemical shifts that have been reported for octahedral Ga^{3+} complexes,

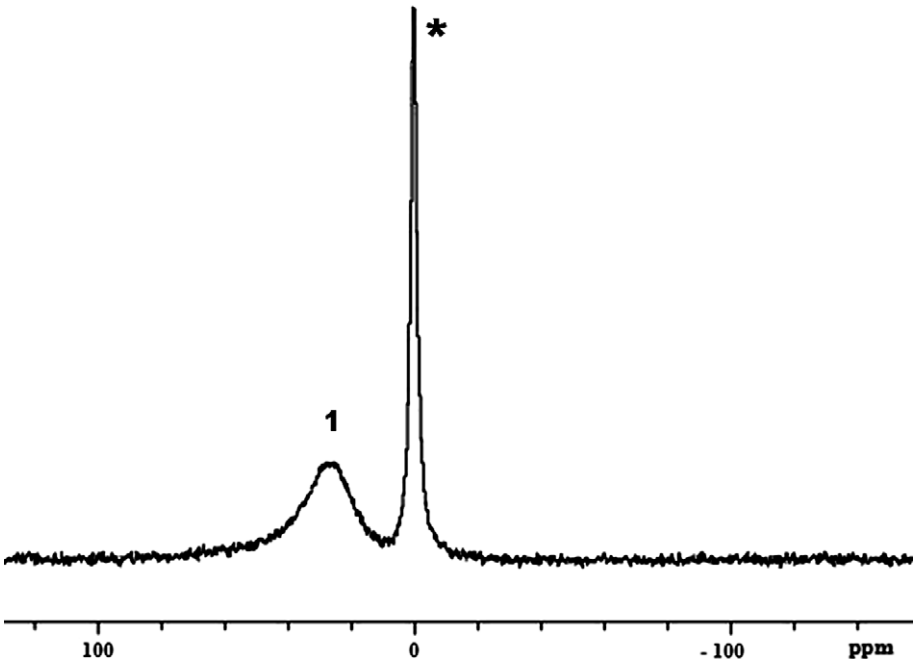

Fig. 3. ^{71}Ga NMR spectrum of **1** in CD_3CN ($^*Ga(H_2O)_6$).

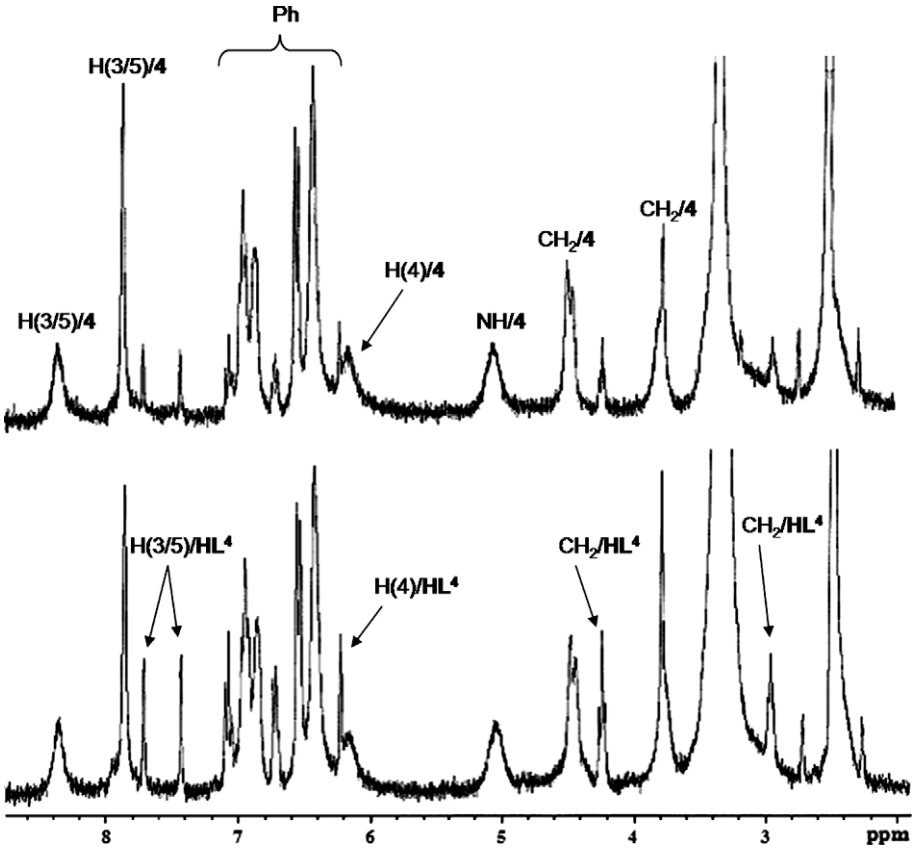

Fig. 4. ^1H NMR spectra of Complex **3** in DMSO-d_6: immediately after preparation of the sample (in the top) and after 24 h in solution at room temperature (in the bottom).

and comparable to values found for other gallium complexes containing phenolate donor groups [19,20].

The ^{1}H NMR spectra of **4**–**6** have always shown the presence of free ligand, even using freshly prepared solutions of the complexes in DMSO-d_6 or CD_3CN. The tendency to release the ligand is more pronounced in dimethyl sulfoxide than in acetonitrile. Due to its limited solubility in most common solvents, the ^{1}H NMR spectrum of **4** could only be recorded in DMSO-d_6. In this solvent, the signals due to the protons of the coordinated ligands are considerably broad (see Fig. 4), which seems to indicate that the complex is undergoing a dynamic process in solution. However, it was not possible to perform variable temperature NMR experiments due to the high freezing point of DMSO-d_6. The ^{1}H NMR spectra of **4**–**6** in DMSO-d_6 have shown the presence of signals assignable to the respective free ligands, immediately after preparation of the samples. In the case of Complex **4**, the proportion of free ligand was 1:2.5 immediately after preparation of the sample, rising to 1:1.5 after 2 h at room temperature and remaining fairly constant (1:1 molar ratio) after 48 and 72 h at room temperature. These data suggest that the complexes may undergo an intermolecular process involving, eventually, the replacement of one of the ancillary ligands by dimethyl sulfoxide molecules. We could not identify signals assignable to any species containing coordinated DMSO, due most probably to the broadness of the spectra. All together, these data indicated that **4**–**6** have a poorer stability in DMSO solution compared with **1**–**3**.

In the case of **5** and **6**, it has been possible to record the respective ^{1}H NMR spectra in CD_3CN. In this solvent, the resonances appear much narrower and with well-resolved multiplicity, being observed three resonances for the pyrazolyl protons, one resonance for the NH protons and six multiplets assignable to the CH_2 protons, integrating each for two protons. These data indicate that both ligands are magnetically equivalent, and also pointed out that the respective methylenic protons are diastereotopic. The magnetic equivalence of the ligands could be accounted by a facial coordination with a symmetrical all-trans configuration of the $N_{pz}N_{am}O_{phen}$ donor atom sets. For Complex **6**, the determination of its solid state structure confirmed the presence of such configuration [$Ga\langle N_{pz1}N_{pz2}\rangle\langle N_{am1}N_{am2}\rangle\langle O_{phen1}O_{phen2}\rangle$] in spite of the poor quality of the crystallographic data. The best crystal measured did not provide a good quality data set to determine a satisfactory structure for **6**. Nevertheless, the connectivity of the atoms was determined unambiguously (compound **6** crystallized from a saturated methanol solution as white crystals in the triclinic space group $P\bar{1}$, with cell parameters $a = 7.8745(4)$ Å, $b = 10.5419(6)$ Å, $c = 18.0674$ Å, $\alpha = 93.784(3)°$, $\beta = 95.814(4)°$, $\gamma = 95.143(3)°$, $V = 5394(3)$ Å^3). Most probably, the configuration found in the solid state for **6** is retained in solution in agreement with the pattern and relative intensity of the peaks observed in the ^{1}H NMR spectra of **5** and **6** in CD_3CN. Compounds **4**–**6** were not characterized by ^{13}C NMR due to their tendency to release slowly the respective ancillary ligands when kept in solution. Using the same conditions as for complexes **1**–**3**, no ^{71}Ga NMR signal could be obtained for **4**–**6**. ^{71}Ga is a quadrupolar nuclei ($I = 3/2$) and the broadening of the line width of ^{71}Ga NMR signals can be due to an exchange process, a change in the correlation time τ_c and the reduction of symmetry about the metal ion [19]. Taking into consideration the behavior observed in solution for complexes **4**–**6** the occurrence of exchange processes is the most plausible possibility to justify the broadening of the line and the absence of ^{71}Ga signals.

3.3. X-ray diffraction analysis of *1*

Suitable crystals of **1** were grown by slow diffusion of diethylether in an acetonitrile solution of the compound. The structure of **1** consists of $[Ga(L^1)_2]^+$ cations and PF_6^- anions that establish several short intermolecular contacts involving hydrogen atoms from the pyrazole and phenoxide rings and fluoride atoms from the counter-ion. An ORTEP diagram of the cation of **1** is shown in Fig. 5 and a selection of bond lengths and angles is presented in Table 2. The coordination geometry around the Ga^{3+} ion is distorted-octahedral. Both ligands are coordinated in a meridional fashion through the oxygen atom from the phenolate group and through the nitrogen atoms from the imine and pyrazole groups. The two pyrazole rings, as well as the two phenoxide groups, exhibit a cis

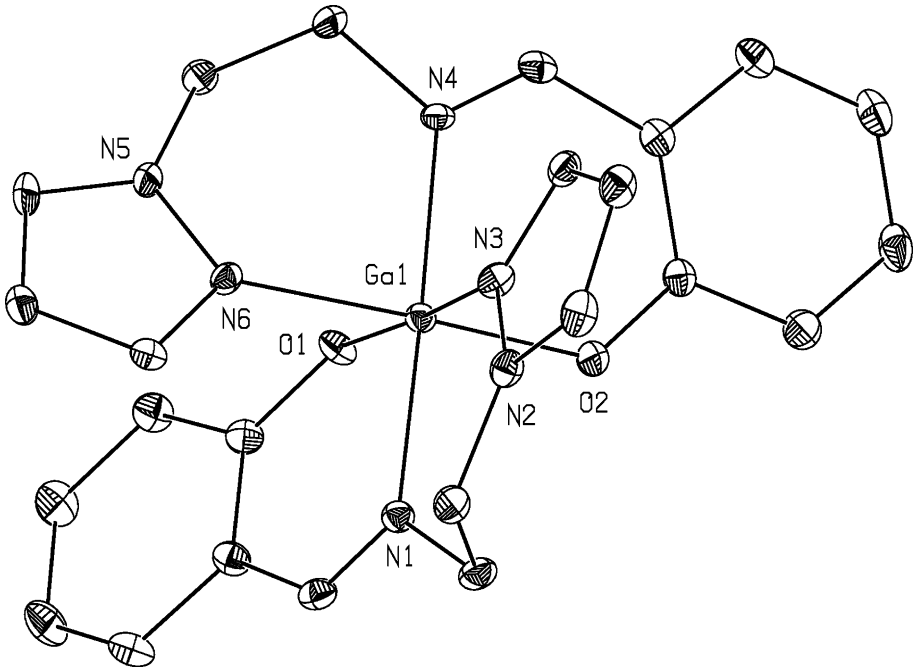

Fig. 5. ORTEP view of Complex **1**; thermal ellipsoids are drawn at the 40% probability level.

Table 2
Selected bond lengths (Å) and angles (°) for $[Ga(L^1)_2]PF_6$ (**1**).

Ga(1)–O(1)	1.920(2)	Ga(1)–O(2)	1.912(2)
Ga(1)–N(1)	2.034(3)	Ga(1)–N(4)	2.047(3)
Ga(1)–N(3)	2.131(3)	Ga(1)–N(6)	2.181(3)
C(1)–O(1)	1.320(4)	C(13)–O(2)	1.308(4)
N(1)–C(7)	1.277(4)	N(1)–C(8)	1.479(4)
N(4)–C(19)	1.285(4)	N(4)–C(20)	1.484(4)
O(1)–Ga(1)–O(2)	96.41(10)	O(1)–Ga(1)–N(1)	91.52(10)
O(1)–Ga(1)–N(3)	174.90(11)	O(1)–Ga(1)–N(4)	89.28.(10)
O(1)–Ga(1)–N(6)	86.18(10)	O(2)–Ga(1)–N(1)	89.11(10)
O(2)–Ga(1)–N(3)	88.67(10)	O(2)–Ga(1)–N(4)	92.83(10)
O(2)–Ga(1)–N(6)	176.75(10)		

orientation, while the imine nitrogen atoms are trans to each other. The cis angles range from 86.2° to 96.4° and the trans angles from 174.9° to 177.8°, which indicates a small distortion of the octahedral geometry as often observed for bis-tridentate Ga(III) complexes. The Ga—O (av. 1.916(2) Å), Ga—N_{im} (av. 2.041(3) Å) and Ga—N_{pz} (av. 2.156(3) Å) bond distances can be considered normal, taking into account the values reported for other Ga(III) complexes containing phenoxide, imine and pyrazole coordinating groups, respectively [5,18,21,22].

3.4. Cytotoxicity in human tumor cell lines

Contrary to complexes **1**–**3**, **4**–**6** tend to undergo exchange processes in DMSO solution with release of the respective ancillary ligands, as discussed above. In addition, the analytical data collected for **4**–**6** could not assess properly the chemical purity of these compounds. Nevertheless, we have pursued with the *in vitro* biological evaluation of **4**–**6** searching to compare their eventual cytotoxic effects with those of **1**–**3**. In these studies, we have not quantified the cytotoxicity of **4**–**6** by IC_{50} measurements which have been performed only for **1**–**3**.

The cytotoxic activity of the Ga(III) complexes (**1–6**) and respective ligands (**HL^1**–**HL^6**) was evaluated in human prostate cancer PC-3 cells and human breast cancer MCF-7 cells, within the concentration range 16 nM–160 μM and using a colorimetric MTT assay. For comparative purposes, such study was also performed for $Ga(NO_3)_3$. Up to a concentration of 160 μM, this gallium salt did not exhibit any cytotoxic effects in both cell lines, being recovered a percentage of viable cells higher than 80% after 24 h of incubation. The Ga complexes (**1**–**6**) and respective ligands (**HL^1**–**HL^6**) have shown a low to moderate cytotoxicity against PC-3 and MCF-7 cells, being **3** and **6** the compounds that have presented the highest ability to induce cell death in both cell lines. Fig. 6 shows the effect of different concentrations (1.6, 32 and 160 μM) of complexes **3** and **6** on the viability of the cells, as well as of the respective free ligands (**HL^3** and **HL^6**) and cisplatin. At the micromolar level (1.6 μM), none of the compounds was able to inhibit the cell growth and the cell viability was not affected. By increasing the concentration of complexes **3** and **6** to 32 μM some cytotoxic effects started already to be observed, which became more pronounced for the highest evaluated concentration of 160 μM. At this concentration, **3** and **6** induced a marked reduction of the cell viability that dropped to values as low as 10% in the case of Complex **6** and for the MCF-7 cell line. Remarkably, **3** and **6** have shown a moderate cytotoxicity against the PC-3 cell line, which has shown a high resistance to cisplatin even at the highest tested concentration (160 μM), as can be seen in Fig. 6.

For complexes **1**–**3** and respective ligands (**HL^1**–**HL^3**), we have measured their IC_{50} values in the PC-3 and MCF-7 cell lines. Such measurements were done after 72 h of incubation and using concentrations of the several compounds in the range 0.32–160 μM. The values determined for the complexes spanned between 13.3 and 108 μM, while those found for the respective ligands ranged between 54 and 223 μM (Table 3). These values confirmed that we were in the presence of weak to moderately cytotoxic compounds, being Complex **3** the one that showed the strongest cytotoxicity in both cell lines.

With the exception of **2** and **HL^2** in MCF-7 cells, the complexation with Ga^{3+} led to a statistically relevant ($p < 0.0001$) enhancement of the cytotoxic potencies of the compounds, according to the following ratios of the respective IC_{50} values: (i) MCF-7 cell line: $IC_{50}(\mathbf{HL^1})/IC_{50}(\mathbf{1}) = 6.0$, $IC_{50}(\mathbf{HL^3})/IC_{50}(\mathbf{3}) = 4.1$; PC-3 cell line: $IC_{50}(\mathbf{HL^1})/IC_{50}(\mathbf{1}) = 2.1$, $IC_{50}(\mathbf{HL^2})/IC_{50}(\mathbf{2}) = 1.6$, $IC_{50}(\mathbf{HL^3})/IC_{50}(\mathbf{3}) = 3.7$. Albeit the observed tendency to obtain lower IC_{50} values for the complexes, the values that have been found for the respective ligands are of the same order of magnitude. Therefore, we can not exclude that the augmented cytotoxic potencies of the complexes could be the result of a stoichiometric effect, reflecting merely the presence of two molecules of ligand per each complex ion [3].

As above discussed, Complex **6** has shown some tendency to release its ancillary ligand of the pyrazole-amine-phenolate type when kept in solution. Hence, one could hypothesize that **6** could undergo dissociation in the extracellular media, releasing the Ga^{3+} cation and the **HL^6** ligands. Being observed such behavior, the biological effects induced by the complex should result from the independent action of their components, i.e. Ga^{3+} and the two **HL^6** ligands. In order to have a better insight into this aspect, we have evaluated the cytotoxicity of Complex **6** against cancer PC-3 cells and human breast cancer MCF-7 cells in the presence of transferrin (500 g/mL of culture medium). This study was run in parallel for $Ga(NO_3)_3$, as well as for Complex **3** that has shown a greater kinetic inertness compared to **6**. The rationale to evaluate the effect of transferrin on the cytotoxic profile of the compounds is justified by the well known ability of this iron transport protein to increase the cellular uptake of Ga^{3+} [23]. The effect of transferrin on the biological action of the compounds was assessed using 1.6, 16 and 80 μM concentrations for complexes **3** and **6** and for $Ga(NO_3)_3$, with molar ratios of the test compounds to transferrin

Table 3
Cytotoxicity of the Ga(III) complexes (**1**–**3**) and their ligands (**HL^1**–**HL^3**) in two human cancer cell lines.

Compound	IC_{50} (μM)[a]	
	MCF-7	PC-3
Ga(III) complexes		
$[Ga(L^1)_2]PF_6$ (1)	37 ± 6	108 ± 21
$[Ga(L^2)_2]PF_6$ (2)	52 ± 13	48 ± 5
$[Ga(L^3)_2]PF_6$ (3)	13.3 ± 3.6	20 ± 4
Ligands		
HL^1	223 ± 29	226 ± 34
HL^2	67 ± 13	75 ± 14
HL^3	54 ± 16	73 ± 24

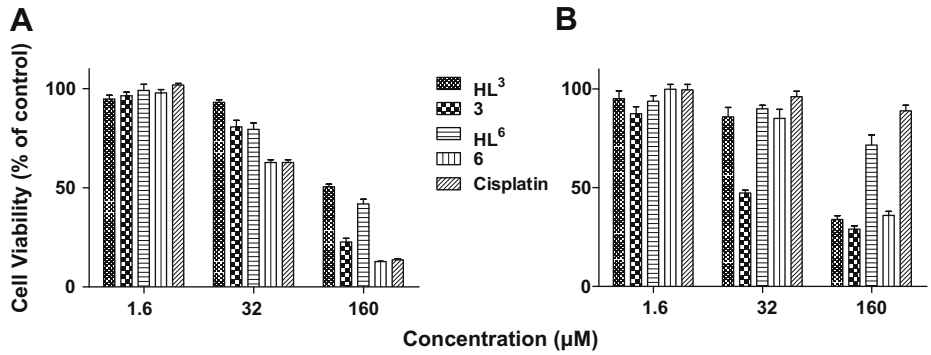

Fig. 6. Effect of the concentration of complexes **3** and **6**, respective ligands (**HL^3** and **HL^6**) and cisplatin on the viability of MCF-7 cells (**A**) and PC-3 cells (**B**).

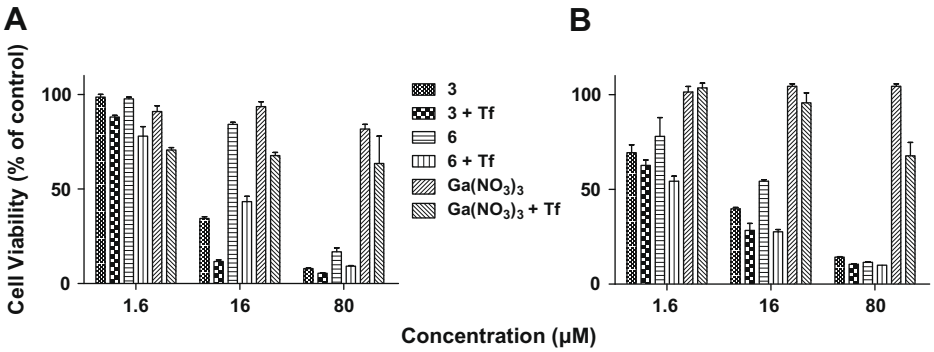

Fig. 7. Effect of the concentration of complexes **3** and **6**, respective ligands (**HL^3** and **HL^6**) and $Ga(NO3)_3$ on the viability of MCF-7 cells (**A**) and PC-3 cells (**B**) in the presence of increasing concentrations of transferrin.

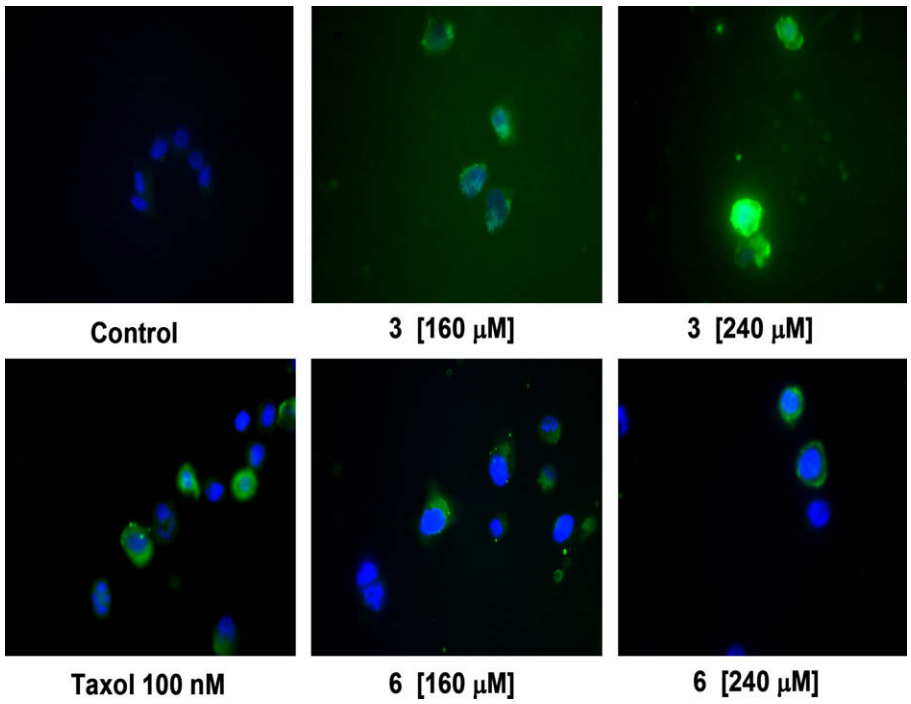

Fig. 8. Images of PC-3 cells after exposure to compounds **3** and **6** for 24 h, with the indicated concentrations, and processed for apoptosis. Staining was performed with FITC-annexin V for apoptotic cells (green) and DAPI for nuclei (blue). Propidium iodide staining (red) was also performed to identify necrotic cells but no signal was present. Taxol was used as a positive control. (For interpretation of the references to colour in this figure legend, the reader is referred to the web version of this article.)

ranging between 1:0.075 and 1:3.75. As can be seen in Fig. 7, in the presence of transferrin the cytotoxic potencies of the complexes were always more pronounced than those of the gallium salt, except when a 1.6 μM concentration of the compounds was tested in the MCF-7 cell line. In general, the presence of transferrin moderately increased the cytotoxicity both for the complexes and gal-

lium nitrate. These finding could be explained by the extracellular dissociation of the complexes and a facilitated transport of the released Ga^{3+} that contributes to increase, although in a relatively low extent, their cytotoxicity potencies. Consistently, the cytotoxicity of the compounds seems to be governed mainly by the pyrazole-containing ligands. However, one cannot exclude that the complexes by themselves have their intrinsic mode of action.

3.5. Evaluation of the induction of apoptosis in human tumor cell lines

Taking into consideration the moderate cytotoxicity exhibited by complexes **3** and **6** and respective ancillary ligands, particularly against the cisplatin-resistant PC-3 cell line, we decide to proceed with the study of their biological activity and we have evaluated if these compounds induced cell death by apoptotic or necrotic processes. Our results show that both **3** and **6** induced cell death through apoptotic processes (Fig 8). The externalization of phosphatidylserine is considered an early event in apoptosis, and can be visualized using the Annexin V protein which displays a high affinity for phosphatidylserine in the presence of Ca^{2+}. The usage of Annexin V–fluorescein conjugates (green signal) allows detection of cells that have initiated apoptotic processes. Our results indicate that both **3** and **6** induced apoptosis at the concentrations evaluated, in agreement with the cytotoxicity results. Necrosis was not observed, since staining with propidium iodide did not elicit any signal. The images presented are merged images from blue (nuclei), green (FITC-annexin V, apoptotic cells) and red (necrotic cells) filters.

4. Conclusions

Chelators of the pyrazole-imine-phenol (**HL^1**–**HL^3**) and pyrazole-amine-phenol (**HL^4**–**HL^6**) type allowed the synthesis of well-defined $[GaL_2]^+$ homoleptic complexes (**1**–**6**). In complexes **1**–**6**, the ligands act as monoanionic and (N,N′,O)-tridentate but display different coordination modes. The more rigid **L^1**–**L^3** coordinate to the Ga^{3+} ion in a meridional fashion (complexes **1**–**3**) while **L^4**–**L^6** are facially coordinated (complexes **4**–**6**). Complexes **1**–**3** have a greater stability in solution compared to **4**–**6**, which have shown a more pronounced tendency to release the respective ancillary ligands. Most probably, such difference reflects the highest rigidity of **L^1**–**L^3**.

The cytotoxicity of **1**–**6** and respective ligands (**HL^1**–**HL^6**) against human prostate cancer cells PC-3 and human breast cancer cells MCF-7 is strongly dependent on the substituents of the phenolate rings. Complexes **3** and **6** that contain chloride substituents at the phenolate rings have shown the highest cytotoxic potency, including in the cisplatin-resistant PC-3 cell line. In both cell lines, **3** and **6** are more cytotoxic than the respective anchor ligands, respectively **HL^1** and **HL^6**, although presenting cytotoxic potencies of the same order of magnitude. It has been also found that the cytotoxic activity of **3** and **6** is slightly increased by the presence of transferrin. All together, these findings could indicate that the enhanced cytotoxicity of the complexes merely reflects a stoichiometric effect and an eventual contribution of the dissociation of the complexes. However, at this point, it can not be excluded that the complexes have their own mode of action.

The induction of cell death by complexes **3** and **6** involves mainly apoptotic processes. Apparently, **3** is a more effective apoptotic inducer. Complex **3**, stabilized by a chloro-substituted pyrazole-imine-phenol ligand, has also shown the highest cytotoxic against a cisplatin-resistant PC-3 cell line. For these reasons, we consider that **3** and related complexes with different halogen substituents (Cl vs. Br vs. I) deserve to be further studied as potential antitumor drugs, in order to elucidate their mechanism of action and identify their molecular target(s). In particular, this should include the evaluation of their capability to act as proteasome inhibitors, since the anticancer properties of other Ga(III) complexes with related asymmetric (N,N′,O)-donor ligands has been recently associated with their ability to inhibit the proteasome activity [9].

Acknowledgement

Francisco Silva wishes to thank the Fundação para a Ciência e Tecnologia (National Foundation for Science and Technology) for a Doctoral research Grants (SFRH/BD/6227/2001). The authors would like to acknowledge FEDER and FCT for financial support (PPCDT/QUI/57632/2004). L. Maria and J. Ascenso are acknowledged for the ^{71}Ga NMR spectroscopic studies. J. Marçalo is acknowledged for the ESI-MS analyzes which were run on a QITMS instrument acquired with the support of the Programa Nacional de Reequipamento Científico (Contract REDE/1503/REM/2005 – ITN) of FCT and is part of RNEM – Rede Nacional de Espectrometria de Massa.

Appendix A. Supplementary material

Supplementary data associated with this article can be found, in the online version, at doi:10.1016/j.jinorgbio.2010.01.003.

References

[1] M.A. Jakupec, M. Galanski, V.B. Arion, C.G. Hartinger, B.K. Keppler, Dalton Trans. (2008) 183–194.
[2] M. Frezza, C.N. Verani, D. Chen, Q.P. Dou, Lett. Drug Des. Discov. 4 (2007) 311–317.
[3] V.B. Arion, M.A. Jakupec, M. Galanski, P. Unfried, B.K. Keppler, J. Inorg. Biochem. 91 (2002) 298–305.
[4] A.V. Rudnev, L.S. Foteeva, C. Kowol, R. Berger, M.A. Jakupec, V.B. Arion, A.R. Timerbaev, B.K. Keppler, J. Inorg. Biochem. 100 (2006) 1819–1826.
[5] R. Shakya, F. Peng, J. Liu, M.J. Heeg, C.N. Verani, Inorg. Chem. 45 (2006) 6263–6268.
[6] A. Dobrov, V.B. Arion, N. Kandler, W. Ginzinger, M.A. Jakupec, A. Rufińska, N.G. Keyserlingk, M. Galanski, C. Kowol, B.K. Keppler, Inorg. Chem. 45 (2006) 1945–1950.
[7] C.R. Kowol, R. Berger, R. Eichinger, A. Roller, M.A. Jakupec, P.P. Schmidt, V.B. Arion, B.K. Keppler, J. Med. Chem. 50 (2007) 1254–1265.
[8] C.R. Kowol, E. Reisner, I. Chiorescu, V.B. Arion, M. Galanski, D.V. Deubel, B.K. Keppler, Inorg. Chem. 47 (2008) 11032–11047.
[9] D. Chen, M. Frezza, R. Shakya, Q.C. Cui, V. Milacic, C.N. Verani, Q.P. Dou, Cancer Res. 67 (2007) 9258–9265.
[10] C. Moura, R.F. Vítor, L. Maria, A. Paulo, I.C. Santos, I. Santos, Dalton Trans. (2006) 5630–5640.
[11] M. Videira, F. Silva, A. Paulo, I.C. Santos, I. Santos, Inorg. Chim. Acta 362 (2009) 2807–2813.
[12] SADABS, Area-Detector Absorption Correction, Brukee AXS Inc., Madison, WI, 2004.
[13] SAINT, Area-Detector Integration Software (Version7.23), Brukee AXS Inc., Madison, WI, 2004.
[14] A. Altomare, M.C. Burla, M. Camalli, G. Cascarano, G. Giacovazzo, A. Guagliardi, A.G.G. Moliterini, G. Polidoro, R.J. Spagna, Appl. Crystallogr. 32 (1999) 115–119.
[15] G.M. Sheldrick, SHELXL-97: Program for the Refinement of Crystal Structure, University of Gottingen, Germany, 1997.
[16] L.J. Farrugia, Appl. Crystallogr. 32 (1999) 837–838.
[17] L.J. Farrugia, ORTEP-3, J. Appl. Crystallogr. 30 (1997) 565.
[18] C. Imbert, H.P. Hratchian, M. Lanznaster, M.J. Heeg, L.M. Hryhorczuk, B.R. McGarvey, H.B. Schlegel, C.N. Verani, Inorg. Chem. 44 (2005) 7414–7422.
[19] J.P. André, H.R. Mäcke, J. Inorg. Biochem. 97 (2003) 315–323.
[20] P. Caravan, C. Orvig, Inorg. Chem. 36 (1997) 236–248.
[21] G. Bandoli, A. Dolmella, F. Tisato, M. Porchia, F. Refosco, Coord. Chem. Rev. 253 (2009) 56–77.
[22] D.L. Reger, Y. Ding, Organometallics 12 (1993) 4485–4492.
[23] C.R. Chitambar, P. Boon, J.P. Wereley, Clin. Cancer Res. 2 (1996) 1009–1015.